

Virialization-induced curvature as a physical explanation for dark energy

Boudewijn F. Roukema,^{1,2} Jan J. Ostrowski,^{1,2} and Thomas Buchert²

¹*Toruń Centre for Astronomy, Faculty of Physics, Astronomy and Informatics,
Nicolaus Copernicus University, ul. Gagarina 11, 87-100 Toruń, Poland*

²*Université de Lyon, Observatoire de Lyon, Centre de Recherche Astrophysique de Lyon, CNRS UMR 5574: Université
Lyon 1 and École Normale Supérieure de Lyon, 9 avenue Charles André, F-69230 Saint-Genis-Laval, France**

(Dated: February 6, 2019)

The geometry of the dark energy and cold dark matter dominated cosmological model (Λ CDM) is commonly assumed to be given by a Friedmann–Lemaître–Robertson–Walker (FLRW) metric, i.e. it assumes homogeneity in the comoving spatial section. The FLRW approximation is expected to fail at (i) small distance scales and (ii) recent epochs. We use the virialization fraction to quantify (i) and (ii), which approximately coincide with each other on the observational past light cone. For increasing time, the virialization fraction increases above 10% at about the same redshift ($\sim 1-3$) at which Ω_Λ grows above 10% (≈ 1.8). Thus, instead of non-zero Ω_Λ , we propose an approximate, general-relativistic correction to the matter-dominated ($\Omega_m = 1, \Omega_\Lambda = 0$), homogeneous metric (Einstein–de Sitter, EdS). A low-redshift effective matter-density parameter of $\Omega_m^{\text{eff}}(0) = 0.26 \pm 0.05$ is inferred. Over redshifts $0 < z < 3$, the distance modulus of the virialization-corrected EdS model approximately matches the Λ CDM distance modulus. This rough approximation assumes “old physics” (general relativity), not “new physics”. Thus, pending more detailed calculations, we strengthen the claim that “dark energy” should be considered as an artefact of emerging average curvature in the void-dominated Universe, via a novel approach that quantifies the relation between virialization and average curvature evolution.

PACS numbers: 98.80.Jk, 04.20.Gz, 02.40.-k

I. INTRODUCTION

It is widely believed that a valid general-relativistic interpretation of recent extragalactic observations, in particular faint galaxy number counts [e.g. 1–3], gravitational lensing [e.g. 4], supernovae type Ia magnitude-redshift relations [e.g. 5, 6]), and the Wilkinson Microwave Anisotropy Probe (WMAP) observations of the cosmic microwave background [7], is that the present-day Universe is dominated by a non-zero dark energy term, modeled in the simplest case by a cosmological constant with today’s value $\Omega_{\Lambda 0} \approx 0.68$ [8]. This interpretation is a consequence of forcing the Friedmann–Lemaître–Robertson–Walker (FLRW) model [9–13], an exact, homogeneous solution of Einstein’s equations, onto the observational data. What are the key assumptions in applying the FLRW model to the data?

One key assumption is an applied mathematics hypothesis, called the “Cosmological Principle” that we rephrase here in a weaker form than usual: a synchronous space-time foliation of the Universe should exist according to which each spatial section can be approximated by a constant-curvature metric on some assumed large *scale of homogeneity*, and the evolution of this metric is given by the homogeneous-isotropic FLRW solution. Since the real Universe is (obviously) inhomogeneous, a second assumption is required: that the cosmic web of filaments, clusters of galaxies and galaxies themselves induce only small perturbations of the perfectly homoge-

neous geometry of the FLRW background. We may think of the background as a *template space-time*, the validity of which should be questioned. (For the question of which background to use and the construction of template metrics employed for the interpretation of observations, see [14–16].)

At what times and length scales are these two assumptions most questionable? They are least accurate at recent times (redshifts $z \lesssim 3$)—since galaxies and large-scale structure have mostly formed recently—and at small ($\ll c/H_0 = 3 h^{-1}$ Gpc) length scales—where structures have had sufficient time to become non-linear and to be bound as virialized objects. The assumption that these structures imply small perturbations of the geometry of the background may be valid for metric perturbations, but it is violated for the derivatives of the metric, in particular for the intrinsic curvature [17].

On the observational past light cone, the recent epoch and small length scale regimes, at which we *expect* that the FLRW solution may fail, approximately coincide.

In the FLRW model, Ω_Λ varies with time. At what epochs is Ω_Λ significantly non-zero, assuming that the present-day value is $\Omega_{\Lambda 0} = 0.68$? Dark energy is significantly non-zero at recent epochs ($z \lesssim 3$).

Hence, the FLRW model should reasonably be *expected* to be a bad approximation on the same scales at which Ω_Λ inferred from applying the FLRW model is significantly non-zero. Since general relativity is well-established empirically on many different scales, the conservative scientific approach is to assume that non-zero dark energy is an artefact of trying to apply the FLRW model in domains where it is expected to fail, unless or until proven otherwise.

* BFR: During visiting lectureship; JJO: During long-term visit.

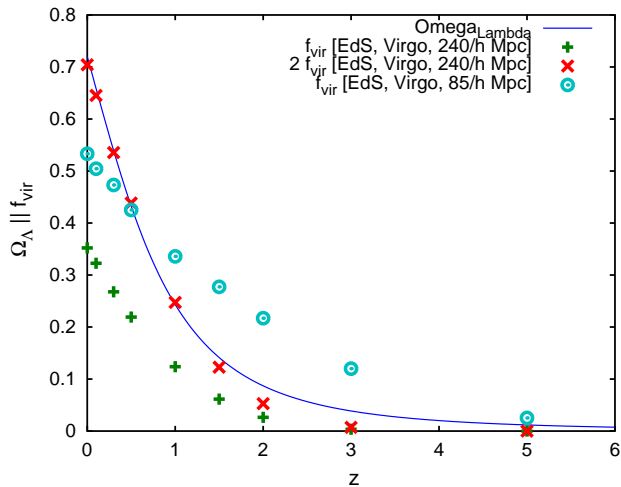


FIG. 1. (colour online) Redshift evolution of Ω_Λ [Eq. (1)] in the Λ CDM model compared to that of the fraction of virialized non-relativistic (non-baryonic plus baryonic) matter, $f_{\text{vir}}(z)$, in EdS 256³-particle Virgo Consortium [18, 19] N -body simulations of box sizes as labelled (see Sect. II A). For comparison with Ω_Λ , $2f_{\text{vir}}$ is also shown for the 240 h^{-1} Mpc simulation.

Can the relation between the scales of the expected failure of the FLRW model and the significantly non-zero values of FLRW-inferred Ω_Λ be quantified? An obvious statistic to quantify the inhomogeneity of the Universe is the fraction of non-relativistic matter (baryonic and non-baryonic matter together) that is contained in virialized (gravitationally bound) systems at a given epoch, $f_{\text{vir}}(z)$. In a flat FLRW model, ignoring radiation density,

$$\begin{aligned} \Omega_\Lambda(z) &= 1 - \Omega_m(z) \\ &= 1 - \frac{\Omega_{m0}H_0^2}{a^3H(z)^2} = 1 - \frac{\Omega_{m0}}{a^3\Omega_{\Lambda0} + \Omega_{m0}}. \end{aligned} \quad (1)$$

Figure 1 shows that on a *linear* redshift scale, the epoch of virialization in an Einstein-de Sitter (EdS, $\Omega_{m0} = 1, \Omega_{\Lambda0} = 0$) model with a cold dark matter (CDM) initial power spectrum (EdS-CDM) coincides closely with the epoch at which Ω_Λ becomes non-negligible in the Concordance Model ([20], Λ CDM), with the details depending on the limitations of the N -body simulations (box size, mass resolution, group-finding algorithms, etc.). The EdS-CDM virialization fraction and the FLRW-inferred dark energy Ω_Λ evolve similarly, to much better than an order of magnitude. Thus, *the FLRW-inferred Ω_Λ dominates the Universe in a way that approximately imitates the degree to which the FLRW geometry should fail*, shown in Fig. 1 for an EdS-CDM model.

How can the virialization fraction and the FLRW-inferred dark energy parameter be more precisely related? Since virialized matter occupies about 1/100-th to 1/200-th of the volume that it would occupy if distributed according to the FLRW background density (e.g.

App. A in [21]), the volume-average of the 3-spatial curvature should become dominated by the curvature corresponding to the volume occupied by the remaining non-virialized matter, generating, on average, negative spatial curvature (if the initial spatial curvature is zero).

In an EdS model the virialization overdensity is, according to a top-hat estimate using the scalar virial theorem for isolated systems,

$$\delta_{\text{vir}} = 18\pi^2 \approx 178, \quad (2)$$

and for low density, zero dark energy models it is bounded below by $8\pi^2$ [21]. Since the curvature is effectively negative, the density of the non-virialized matter inferred from assuming zero curvature is an overestimate. Since matter mostly flows out of voids, the rate of expansion (Hubble parameter) in the majority of the volume, i.e. in non-virialized low-density regions, is higher than the background model average expansion rate. Again, the matter density parameter, inferred from assuming a homogeneous Hubble parameter, is overestimated in comparison to calculating it in proportion to the critical density of the non-virialized region itself. Thus, the degree of negative curvature is underestimated both due to curvature itself and due to deviations in the expansion rate, which can be condensed into a single \mathcal{X} -matter parameter (see below).

The scalar averaging approach to relativistic, inhomogeneous models of the Universe [e.g. 14, 22–25], focuses on the kinematical backreaction, $\Omega_{\mathcal{Q}}^{\mathcal{D}}(z) \equiv -\mathcal{Q}_{\mathcal{D}}/(6H_{\mathcal{D}}^2)$, and the average curvature parameter $\Omega_{\mathcal{R}}^{\mathcal{D}}(z) \equiv -\langle \mathcal{R} \rangle_{\mathcal{D}}/(6H_{\mathcal{D}}^2)$, where $H_{\mathcal{D}}$ is the volume-averaged Hubble rate within a spatial compact domain \mathcal{D} . The former is an averaged expression of extrinsic curvature invariants, which can be interpreted kinematically and depend (in general) on the variance in the expansion rate and the averaged rates of shear and vorticity, while the latter represents the average scalar curvature (3-Ricci curvature) over the domain \mathcal{D} . The overall backreaction effect can be condensed into an \mathcal{X} -matter parameter, defined $\Omega_{\mathcal{X}}^{\mathcal{D}}(z) := \Omega_{\mathcal{Q}}^{\mathcal{D}}(z) + \Omega_{\mathcal{R}}^{\mathcal{D}}(z)$ and obeying the Hamilton constraint on the averaged density parameters

$$\Omega_m^{\mathcal{D}}(z) + \Omega_{\mathcal{X}}^{\mathcal{D}}(z) + \Omega_\Lambda^{\mathcal{D}}(z) = 1, \quad (3)$$

where $\Omega_\Lambda^{\mathcal{D}} := \Lambda/(3H_{\mathcal{D}}^2)$ is the volume-averaged dark energy parameter.

Earlier calculations, starting with a homogeneous EdS background model, suggest that the peculiar curvature parameter, i.e. the deviation of the total averaged 3-Ricci curvature from a constant-curvature model, $\Omega_{\mathcal{W}}^{\mathcal{D}}(z) := -\mathcal{W}_{\mathcal{D}}/6H_{\mathcal{D}}^2$, with $\mathcal{W}_{\mathcal{D}} := \langle \mathcal{R} \rangle_{\mathcal{D}} - 6k/a^2$, has a much stronger (a factor of about 5) effect than the kinematical backreaction $\Omega_{\mathcal{Q}}^{\mathcal{D}}(z)$ (cf. Figs 3, 4 in [22]). Thus, the use of virialization to calculate more realistic estimates of the average scalar curvature and its evolution should provide an approximate, general-relativistic space-time model that is more accurate than the FLRW model. This effective-metric model is not expected to satisfy the Einstein equation on any given (recent) time slice [16]. Thus,

the effective metric presented below (38) is unlikely to be consistent with the Lemaitre–Tolman–Bondi (LTB) model [26–28], which has recently been parametrized against observations [29, 30].

The approximation method proposed here, for an EdS background model, is described in Sect. II and the results are presented in Sect. III. An OCTAVE script for making the calculations and plots is provided in the source package for the preprint version of this paper[31]. Conclusions are given in Sect. V.

II. THE VIRIALIZATION APPROXIMATION

A. N -body simulations

“Dark” (i.e. baryonic plus non-baryonic) matter halo merger history trees have been calculated since 1992 from N -body simulations [32, 33] and by semi-analytical methods [34]. Estimates of the virialization fraction are implied by these calculations, e.g. Table 6 in [35]. Here, the N -body simulations used are Virgo Consortium 256^3 -particle T^3 (3-torus) simulations [18, 19, 36] for an EdS-CDM model with $h = 0.5$, and normalization in the mean density fluctuation $\sigma_8 = 0.51$ at $8h^{-1}$ Mpc, where the Hubble constant, i.e. the zero redshift Hubble parameter, is written $H_0 \equiv 100h$ km/s/Mpc. One simulation has comoving box size $239.5 h^{-1}$ Mpc and mass per dark matter particle (implicitly, baryonic and non-baryonic together) of $m = 2.27 \times 10^{11} h^{-1} M_\odot$, the other $84.55 h^{-1}$ Mpc and $m = 1.0 \times 10^{10} h^{-1} M_\odot$. The length scale of the latter simulation is small, so the simulation is only used for comparison in Fig. 1. A friends-of-friend group finder FOF-1.1[36] at 0.2 times the mean interparticle separation, for a minimum of 8 particles per group, i.e. $1.8 \times 10^{12} h^{-1} M_\odot$, is used independently at each output redshift z to detect virialized objects at that redshift, giving the number of virialized particles N_{vir} and the complement, i.e. the number of non-virialized particles $N - N_{\text{vir}}$, where $N = 256^3$ is the total number of particles. A different group finder, such as a spherical overdensity (SO) group finder, would give somewhat different results to those found here [37–39], but since we are interested in the total virialized mass, the dilemma of whether to define a slightly overlapping pair of haloes as a single halo (FOF) or a pair of dynamically distinct haloes (SO) is insignificant for the present work. We define the virialization fraction

$$f_{\text{vir}}(z) := \frac{N_{\text{vir}}(z)}{N}. \quad (4)$$

We spline interpolate between simulation output times.

B. Effective cosmological parameters

The effective, i.e. volume-averaged, matter density parameter combines the matter density parameter in the

non-virialized region with that in the (at late times) much tinier virialized region. If we think of the particles in their original comoving positions in the background model, then the volumes occupied by the two regions are approximately in the ratio $(1 - f_{\text{vir}}) : f_{\text{vir}}$. However, taking into account the actual situation of a virialized region, we notice that the volume occupied by the virialized matter has shrunk by a factor of about δ_{vir} (2), so in the homogeneous model (with no local nor comoving global curvature changes), the volume ratio increases to $(1 - f_{\text{vir}}/\delta_{\text{vir}}) : f_{\text{vir}}/\delta_{\text{vir}}$. Following, e.g., [23, 40], let us label the non-virialized and virialized regions \mathcal{E} (for “empty”) and \mathcal{M} (for “massive”), respectively, and their disjoint union $\mathcal{D} := \mathcal{M} \cup \mathcal{E}$. We now establish a general formalism in Sect. IIB 1, derive formulae for the dark-energy-free, stable clustering case in Sect. IIB 2, and describe how to use these in Sect. IIB 3.

1. General formulae

Writing $|\mathcal{F}|$ for the volume of a spatial region \mathcal{F} , let us define $\lambda_{\mathcal{M}} := |\mathcal{M}|/|\mathcal{D}|$. This corresponds to the virialization volume fraction, with $\lambda_{\mathcal{M}} := f_{\text{vir}}/\delta_{\text{vir}}$. As in (25) of [23], we then have the linear combinations

$$H_{\mathcal{D}} = \lambda_{\mathcal{M}} H_{\mathcal{M}} + (1 - \lambda_{\mathcal{M}}) H_{\mathcal{E}} \quad (5)$$

$$\langle \rho \rangle_{\mathcal{D}} = \lambda_{\mathcal{M}} \langle \rho \rangle_{\mathcal{M}} + (1 - \lambda_{\mathcal{M}}) \langle \rho \rangle_{\mathcal{E}} \quad (6)$$

$$\langle \mathcal{R} \rangle_{\mathcal{D}} = \lambda_{\mathcal{M}} \langle \mathcal{R} \rangle_{\mathcal{M}} + (1 - \lambda_{\mathcal{M}}) \langle \mathcal{R} \rangle_{\mathcal{E}}. \quad (7)$$

As shown in [23], the the volume-averaged Hamiltonian constraint,

$$3H_{\mathcal{D}}^2 = 8\pi G \langle \varrho \rangle_{\mathcal{D}} - \frac{1}{2} \langle \mathcal{R} \rangle_{\mathcal{D}} - \frac{1}{2} \mathcal{Q}_{\mathcal{D}} + \Lambda, \quad (8)$$

leads to the kinematical backreaction on \mathcal{D} ,

$$\begin{aligned} \mathcal{Q}_{\mathcal{D}} &= \lambda_{\mathcal{M}} \mathcal{Q}_{\mathcal{M}} + (1 - \lambda_{\mathcal{M}}) \mathcal{Q}_{\mathcal{E}} \\ &+ 6\lambda_{\mathcal{M}} (1 - \lambda_{\mathcal{M}}) (H_{\mathcal{M}} - H_{\mathcal{E}})^2. \end{aligned} \quad (9)$$

As in [40], we may now define cosmological parameters on \mathcal{D} using (8). Similarly to the FLRW model, these are derived by dividing (8) by $3H_{\mathcal{D}}^2$. For a generic spatial domain \mathcal{F} , which may be any of \mathcal{D} , \mathcal{M} , or \mathcal{E} , we define the cosmological parameters

$$\begin{aligned} \Omega_m^{\mathcal{F}} &:= \frac{8\pi G}{3H_{\mathcal{D}}^2} \langle \varrho \rangle_{\mathcal{F}}, \quad \Omega_\Lambda^{\mathcal{F}} := \frac{\Lambda}{3H_{\mathcal{D}}^2}, \\ \Omega_{\mathcal{R}}^{\mathcal{F}} &:= -\frac{\langle \mathcal{R} \rangle_{\mathcal{F}}}{6H_{\mathcal{D}}^2}, \quad \Omega_{\mathcal{Q}}^{\mathcal{F}} := -\frac{\mathcal{Q}_{\mathcal{F}}}{6H_{\mathcal{D}}^2}. \end{aligned} \quad (10)$$

The choice of dividing by $H_{\mathcal{D}}^2$ independently of the choice of \mathcal{F} is motivated by the stable clustering hypothesis [41], according to which the averaged expansion rate in \mathcal{M} (virialized regions) is zero, i.e. $H_{\mathcal{M}} \approx 0$.

With these definitions, the Hamiltonian constraint (8) on \mathcal{F} is

$$\Omega_m^{\mathcal{F}} + \Omega_\Lambda^{\mathcal{F}} + \Omega_{\mathcal{R}}^{\mathcal{F}} + \Omega_{\mathcal{Q}}^{\mathcal{F}} = \frac{H_{\mathcal{F}}^2}{H_{\mathcal{D}}^2}. \quad (11)$$

Thus, the dimensionless parameters Ω defined this way sum to unity on the combined domain \mathcal{D} , but on \mathcal{M} or \mathcal{E} are only constrained to sum to a non-negative value, which is determined by comparing the region's squared expansion rate to that of the combined domain \mathcal{D} .

2. Dark-energy-free, stable clustering case

Let us assume no dark energy, i.e. $\Lambda = 0$, and the stable clustering hypothesis for the \mathcal{M} regions, $H_{\mathcal{M}} \approx 0$. Thus (5) becomes

$$H_{\mathcal{D}} = (1 - \lambda_{\mathcal{M}}) H_{\mathcal{E}}. \quad (12)$$

Using (12), (6), (7), (9), and (10) we find that the average characteristics are related:

$$\begin{aligned} \Omega_m^{\mathcal{D}} &= (1 - \lambda_{\mathcal{M}}) \Omega_m^{\mathcal{E}} + \lambda_{\mathcal{M}} \Omega_m^{\mathcal{M}}; \\ \Omega_{\mathcal{R}}^{\mathcal{D}} &= \lambda_{\mathcal{M}} \Omega_{\mathcal{R}}^{\mathcal{M}} + (1 - \lambda_{\mathcal{M}}) \Omega_{\mathcal{R}}^{\mathcal{E}}; \\ \Omega_{\mathcal{Q}}^{\mathcal{D}} &= \lambda_{\mathcal{M}} \Omega_{\mathcal{Q}}^{\mathcal{M}} + (1 - \lambda_{\mathcal{M}}) \Omega_{\mathcal{Q}}^{\mathcal{E}} - \frac{\lambda_{\mathcal{M}}}{1 - \lambda_{\mathcal{M}}}. \end{aligned} \quad (13)$$

The Hamiltonian constraint in the form (11) gives three independent equilibria,

$$\begin{aligned} \Omega_m^{\mathcal{D}} + \Omega_{\mathcal{R}}^{\mathcal{D}} + \Omega_{\mathcal{Q}}^{\mathcal{D}} &= 1; \\ \Omega_m^{\mathcal{M}} + \Omega_{\mathcal{R}}^{\mathcal{M}} + \Omega_{\mathcal{Q}}^{\mathcal{M}} &= 0; \\ \Omega_m^{\mathcal{E}} + \Omega_{\mathcal{R}}^{\mathcal{E}} + \Omega_{\mathcal{Q}}^{\mathcal{E}} &= \frac{1}{(1 - \lambda_{\mathcal{M}})^2}. \end{aligned} \quad (14)$$

Together, (13) and (14) consist of, at a given redshift z , six algebraic equations with nine unknowns, where the virialization volume fraction $\lambda_{\mathcal{M}}(z)$ is estimated by calculating $f_{\text{vir}}(z)$ from a background model (4) and by using the appropriate analytical value of δ_{vir} for that model. This set of equations should be used along with the void-dominated expansion rate (12), since $H_{\mathcal{D}}$ is used in defining these Ω parameters. These formulae are valid at each redshift.

To retain generality while simplifying the algebra, we introduce the sums

$$\Omega_{\mathcal{R}}^{\mathcal{F}} + \Omega_{\mathcal{Q}}^{\mathcal{F}} =: \Omega_X^{\mathcal{F}}, \quad (15)$$

so that we can consider X matter to represent the deviation of the averaged parameters from FLRW behavior. Thus, six variables are reduced to three, while equations (7) and (9) become a single equation. The resulting set

of equations is

$$\Omega_m^{\mathcal{D}} = (1 - \lambda_{\mathcal{M}}) \Omega_m^{\mathcal{E}} + \lambda_{\mathcal{M}} \Omega_m^{\mathcal{M}} \quad (16)$$

$$\Omega_X^{\mathcal{D}} = \lambda_{\mathcal{M}} \Omega_X^{\mathcal{M}} + (1 - \lambda_{\mathcal{M}}) \Omega_X^{\mathcal{E}} - \frac{\lambda_{\mathcal{M}}}{1 - \lambda_{\mathcal{M}}} \quad (17)$$

$$\Omega_m^{\mathcal{D}} + \Omega_X^{\mathcal{D}} = 1 \quad (18)$$

$$\Omega_m^{\mathcal{M}} + \Omega_X^{\mathcal{M}} = 0 \quad (19)$$

$$\Omega_m^{\mathcal{E}} + \Omega_X^{\mathcal{E}} = \frac{1}{(1 - \lambda_{\mathcal{M}})^2}, \quad (20)$$

where (20) is redundant, since it is implied by (16)–(19). Thus, there are four independent algebraic relations with six unknowns, given the virialization volume fraction $\lambda_{\mathcal{M}}$.

3. Background model

The equations in Sect. II B 1 could, in principle, be solved in a background-free way. Here, we use a background FLRW model to approximate the void region matter density parameter

$$\begin{aligned} \Omega_m^{\mathcal{E}} &= \frac{8\pi G}{3H_{\mathcal{D}}^2} \langle \rho \rangle_{\mathcal{E}} \approx \frac{8\pi G}{3H_{\mathcal{D}}^2} (1 - f_{\text{vir}}) \langle \rho \rangle^{\text{bg}} \\ &= (1 - f_{\text{vir}}) \left(\frac{H^{\text{bg}}}{H_{\mathcal{D}}} \right)^2 \Omega_m^{\text{bg}}, \end{aligned} \quad (21)$$

where $\langle \rho \rangle^{\text{bg}}$, Ω_m^{bg} , and H^{bg} are the FLRW mean density, density parameter, and expansion rate, respectively. Here, we have assumed that since $f_{\text{vir}} < 1$ and $\delta_{\text{vir}} \approx 178$ [EdS case, (2)], we have $\lambda_{\mathcal{M}} \ll 1$, so that the non-virialized matter occupies approximately the full volume. The virialized matter density parameter can also be estimated from the background model,

$$\begin{aligned} \Omega_m^{\mathcal{M}} &= \frac{8\pi G}{3H_{\mathcal{D}}^2} \langle \rho \rangle_{\mathcal{M}} \approx \frac{8\pi G}{3H_{\mathcal{D}}^2} \delta_{\text{vir}} \langle \rho \rangle^{\text{bg}} \\ &= \delta_{\text{vir}} \left(\frac{H^{\text{bg}}}{H_{\mathcal{D}}} \right)^2 \Omega_m^{\text{bg}}. \end{aligned} \quad (22)$$

Thus, substituting (21) and (22) into (16) gives

$$\begin{aligned} \Omega_m^{\text{eff}}(z) &:= \Omega_m^{\mathcal{D}} \approx \left[1 - \frac{f_{\text{vir}}}{\delta_{\text{vir}}} (1 - f_{\text{vir}}) \right] \left(\frac{H^{\text{bg}}}{H^{\text{eff}}} \right)^2 \Omega_m^{\text{bg}} \\ &\approx \left(\frac{H^{\text{bg}}}{H^{\text{eff}}} \right)^2 \Omega_m^{\text{bg}}, \end{aligned} \quad (23)$$

where the \mathcal{D} -averaged parameter has been relabeled as an effective parameter. For percent-level accuracy, the first line in (23) is necessary, though not sufficient.

When assuming a background EdS model, the effective expansion rate implied by the stable clustering hypothesis, i.e. using (12), combines the background, time-varying expansion rate $H^{\text{bg}}(z)$ with the peculiar expansion rate expressed as a velocity difference normalized by

a comoving spatial separation, $H_{\text{pec}}^{\text{com}}(z)$,

$$\begin{aligned} H^{\text{eff}}(z) &:= H_{\mathcal{D}} \\ &= (1 - \lambda_{\mathcal{M}}) [H^{\text{bg}}(z) + H_{\text{pec}}^{\text{com}}(z) a^{-1}], \end{aligned} \quad (24)$$

where the a^{-1} factor converts the peculiar expansion rate from comoving to physical length units. At redshifts prior to the virialization epoch, i.e. for $z \gtrsim 3$, we must have

$$H^{\text{eff}}(z) \approx H^{\text{bg}}(z). \quad (25)$$

This is given by the homogeneous Friedmann equation,

$$H^{\text{bg}}(z) = H_0^{\text{bg}} \sqrt{\Omega_{\Lambda 0}^{\text{bg}} + \Omega_{k 0}^{\text{bg}} a^{-2} + \Omega_{m 0}^{\text{bg}} a^{-3}}, \quad (26)$$

for background model zero-redshift parameters including (in general) the Hubble constant (H_0^{bg}), and the dark energy ($\Omega_{\Lambda 0}^{\text{bg}}$), curvature ($\Omega_{k 0}^{\text{bg}}$), and matter density ($\Omega_{m 0}^{\text{bg}}$) parameters. In a comoving-rigid void model (i.e. a standard FLRW model), these background parameters correspond to zero-redshift parameters. In the virialization approximation, these parameters only exist as hypothetical projections from high redshift to an idealized low-redshift state; they are not physically realized. In the present work, we only consider an EdS background model, so (26) simplifies to

$$H^{\text{bg}}(z) = H_0^{\text{bg}} a^{-3/2}. \quad (27)$$

In order to match low redshift estimates, the background model Hubble constant H_0^{bg} should be set so that the virialization approximation zero-redshift value

$$H^{\text{eff}}(0) = \left[1 - \frac{f_{\text{vir}}(0)}{\delta_{\text{vir}}} \right] [H_0^{\text{bg}} + H_{\text{pec}}^{\text{com}}(0)] \quad (28)$$

[cf. (24) and (27)] matches recent low redshift estimates of H_0 (Sect. II C).

Estimating $H_{\text{pec}}^{\text{com}}(z)$ from background N -body simulations would be difficult with standard T^3 FLRW simulations, since the average velocity difference is calculated along a straight closed curve γ across the simulation box, i.e. it is zero by construction. Thus, here, we estimate $H_{\text{pec}}^{\text{com}}(0)$ from observations (Sect. II C). Determining the redshift dependence $H_{\text{pec}}^{\text{com}}(z)$ directly from observations would be more difficult and model-dependent. However, we have two known constraints: (25) and (28) must be satisfied at the high and low redshift limits, respectively. At the high redshift limit, a smooth transition at high redshifts seems physically reasonable. Moreover, virialization cannot occur without reducing the matter density in the voids. As the voids become more and more empty, the imbalance in gravitational potential between the centre and edge of a void becomes stronger and stronger. Thus, it is physically likely that $H_{\text{pec}}^{\text{com}}(z)$ increases monotonically as $f_{\text{vir}}(z)$ increases (i.e. as z decreases). Here,

we propose a functional form for $H_{\text{pec}}^{\text{com}}(z)$ proportional to the virialization fraction, i.e.

$$H_{\text{pec}}^{\text{com}}(z) = H_{\text{pec}}^{\text{com}}(0) \frac{f_{\text{vir}}(z)}{f_{\text{vir}}(0)}. \quad (29)$$

By definition, this formula satisfies the high and low redshift limits, has a smooth high-redshift transition, and has $H_{\text{pec}}^{\text{com}}(z)$ increasing monotonically as $f_{\text{vir}}(z)$ increases. Checking the detailed shape of this function should be considered as both an observational and a theoretical test of the hypothesis that the EdS model is the correct background model. Neither task is trivial, however, since both need to be done in the framework of the scalar averaging approach (e.g., using the relativistic Zel'dovich approximation [24, 25]), rather than in the perturbed FLRW framework.

Since we assume zero dark energy in our background model and we approximate $\Omega_{\mathcal{Q}}^{\mathcal{D}}(z)$ as small, (18), (3), and (15) give the effective sign-reversed curvature parameter

$$\Omega_{\mathcal{R}}^{\text{eff}}(z) = 1 - \Omega_{\text{m}}^{\text{eff}}(z), \quad (30)$$

where \mathcal{D} -averaged parameters are again relabeled as effective parameters. The effective comoving curvature radius at a given epoch can now be written

$$R_{\mathcal{C}}^{\text{eff}}(z) = \frac{c}{a H^{\text{eff}}(z)} \frac{1}{\sqrt{\Omega_{\mathcal{R}}^{\text{eff}}(z)}}, \quad (31)$$

where for simplicity, we assume that $\Omega_{\mathcal{R}}^{\text{eff}} > 0 \forall z$.

Using (27), we can rewrite the first line of (23) for the EdS case as

$$\Omega_{\text{m}}^{\text{eff}}(z) \approx \left[1 - \frac{f_{\text{vir}}}{\delta_{\text{vir}}} (1 - f_{\text{vir}}) \right] \left(\frac{H_0^{\text{bg}}}{H^{\text{eff}}} \right)^2 a^{-3}, \quad (32)$$

i.e., an effective matter density parameter that is clearly less than unity during the virialization epoch.

C. Observational assumptions

Two low-redshift limit observational estimates are needed in order to evaluate (24). We adopt

$$H^{\text{eff}}(0) = 74.0 \pm 1.6 \text{ km/s/Mpc} \quad (33)$$

using the recent low-redshift Hubble constant estimates of $H_0 = 73.8 \pm 2.4 \text{ km/s/Mpc}$ [42] and $H_0 = 74.3 \pm 2.1 \text{ km/s/Mpc}$ [43].

To estimate the present value of the peculiar expansion rate $H_{\text{pec}}^{\text{com}}(0)$, we divide the typical infall velocity v_{infall} around rich clusters of galaxies by the typical void radius $D_{\text{void}}/2$, where both are for low redshift data. Out to a distance of $130h^{-1} \text{ Mpc}$ and at 10 or more degrees above the Galactic Plane, the median size of eight voids found in the IRAS Point Source Catalog redshift survey

(IRAS/PSCz) is $D_{\text{void}}/2 = 28.3 h^{-1}$ Mpc [44]. In Data Release 5 of the Sloan Digital Sky Survey (SDSS), a much larger sample of 222 voids found in the redshift range $0.04 < z < 0.16$ in a solid angle of about 2300 deg^2 has a mean comoving void radius of

$$D_{\text{void}}/2 \approx 25 \pm 2 h^{-1} \text{ Mpc} \quad (34)$$

([45]; standard error by inspection of Fig. 4).

Infall velocities are not normally derived from observations with the aim of estimating $H_{\text{pec}}^{\text{com}}$. The Cluster and Infall Region Nearby Survey (CAIRNS) study of nine low-redshift rich clusters gives a caustic outline for infall velocities in front and behind the clusters of about

$$v_{\text{infall}} \approx 2\sigma_v, \quad (35)$$

where σ_v is the line-of-sight velocity dispersion of cluster galaxies (Fig. 4, [46], within one sky-plane virial radius of the cluster centers). See [47] for a discussion of redshift space effects interpreted using a homogeneous model, especially Fig. 5 illustrating caustics related to the turnaround radius. Velocity dispersions of 91 rich clusters of the ESO Nearby Abell Cluster Survey (ENACS) and earlier surveys selected out to $z = 0.1$ from a solid angle of $\approx 8400 \text{ deg}^2$ have a mean of $\sigma_v = 642 \pm 24 \text{ km/s}$ (Table 1a, [48]; standard error in the mean; cf Fig. 5a of [48]). An SDSS Data Release 4 analysis of 109 clusters out to $z < 0.1$ over 6700 deg^2 yields $\sigma_v = 585 \pm 15 \text{ km/s}$ (Table 1, [49]; standard error in the mean). The two catalogues have very few members in common, so an inverse-variance weighted mean can be calculated:

$$\sigma_v = 601 \pm 13 \text{ km/s}. \quad (36)$$

Thus, with $h = 0.74$ from (33) and using (34), (35), and (36) we set

$$H_{\text{pec}}^{\text{com}}(0) := \frac{2v_{\text{infall}}}{D_{\text{void}}} \approx \frac{4\sigma_v}{D_{\text{void}}} = 36 \pm 3 \text{ km/s/Mpc}. \quad (37)$$

D. Effective metric

We extend the usual FLRW metric to an effective, spherically symmetric, comoving, observer-centred expression for the metric:

$$ds^2 = -c^2 dt^2 + a^2(t) \left[d\chi^{\text{eff}2} + R_C^{\text{eff}2} \sinh^2 \frac{\chi^{\text{eff}}}{R_C^{\text{eff}}} (d\theta^2 + \cos^2 \theta d\phi^2) \right], \quad (38)$$

where the differential radial comoving distance is

$$d\chi^{\text{eff}}(z) = \frac{c dt}{a} = \frac{c dt}{a da} da = \frac{c}{a^2 H^{\text{eff}}(z)} da, \quad (39)$$

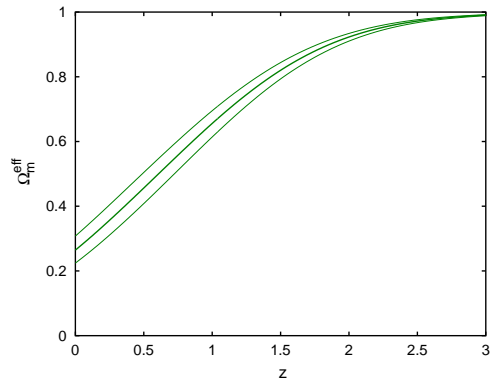


FIG. 2. Effective zero redshift matter density parameter Ω_m^{eff} (32) in the virialization approximation. The upper, central, and lower curves correspond to $H_{\text{pec}}^{\text{com}}(0) = 33, 36,$ and 39 km/s/Mpc , respectively [see (37)].

and c is the conversion constant between space and time units. Equation (39) can be integrated numerically to obtain χ^{eff} and the luminosity distance

$$d_L^{\text{eff}}(z) = (1+z) R_C^{\text{eff}} \sinh \frac{\chi^{\text{eff}}}{R_C^{\text{eff}}}. \quad (40)$$

The effective differential volume element per square degree, necessary for faint galaxy number count analyses, is

$$\frac{dV^{\text{eff}}}{dz}(z) = \left(\frac{\pi}{180} \right)^2 R_C^{\text{eff}2} \sinh^2 \frac{\chi^{\text{eff}}}{R_C^{\text{eff}}} \frac{d\chi^{\text{eff}}}{dz}. \quad (41)$$

The luminosity distance for the virialization approximation and for the homogeneous EdS and Λ CDM models can be normalized to the Milne model for convenience, yielding distance moduli $m - M$. The fraction of the distance modulus that would be needed to correct the homogeneous EdS model to match the Λ CDM model can be written as follows:

$$f_{m-M} := \frac{\log_{10} d_L^{\text{eff}} - \log_{10} d_L^{\text{EdS}}}{\log_{10} d_L^{\Lambda\text{CDM}} - \log_{10} d_L^{\text{EdS}}}. \quad (42)$$

III. RESULTS

The virialization fraction f_{vir} from the two N -body simulations has already been shown in Fig. 1. Figure 2 shows that, as expected, the effective matter density parameter contributing to curvature drops as the redshift decreases to zero. The low redshift value, $\Omega_m^{\text{eff}}(0) = 0.26 \pm 0.05$, is impressively close to observational low redshift estimates of $\Omega_m \sim 0.3$. It is *not* a result of fitting the virialization approximation to observational data. Apart from assuming an EdS background model, the only observational values used in the formulae above are those presented in Sect. II C, i.e. $H^{\text{eff}}(0)$ (28) and $H_{\text{pec}}^{\text{com}}(0)$

TABLE I. N -body simulation estimates of $f_{\text{vir}}(z)$ (4)

z	10.0	5.0	3.0	2.0	1.5	1.0	0.5	0.3	0.1	0.0
f_{vir}	0	1.4×10^{-5}	0.0036	0.026	0.061	0.12	0.22	0.27	0.32	0.35

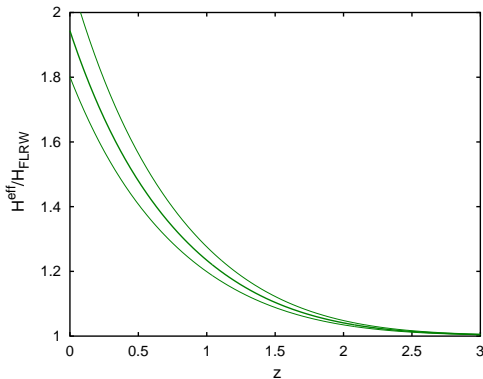


FIG. 3. Ratio of effective to background expansion rates $H^{\text{eff}}(z)/H(z)$, using (24), (27), and (28). The upper, central, and lower curves correspond to $H_{\text{pec}}^{\text{com}}(0) = 39, 36$, and 33 km/s/Mpc, respectively.

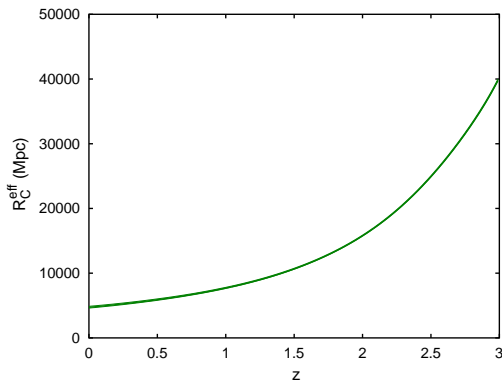


FIG. 4. Effective comoving curvature radius R_C^{eff} (31) in the virialization approximation. The uncertainty in $H_{\text{pec}}^{\text{com}}(0)$ is not visible in this plot.

(37). Figure 3 shows the effective expansion rate evolution, which, along with f_{vir} , explains the lower effective matter density parameter at low redshifts. Through the comoving curvature radius (31), the void-dominated expansion rate at low redshifts also leads to stronger negative average curvature, by decreasing R_C^{eff} . Figure 4 shows the effective curvature radius evolution $R_C^{\text{eff}}(z)$.

Figure 5 shows that applying the virialization approximation to the EdS model brings the EdS distance modulus close to the (homogeneous) Λ CDM distance modulus. The fraction f_{m-M} (42) provided by the virialization approximation is shown in Fig. 6, showing that a discrepancy remains for $z < 1$. Figure 7 shows that the volume

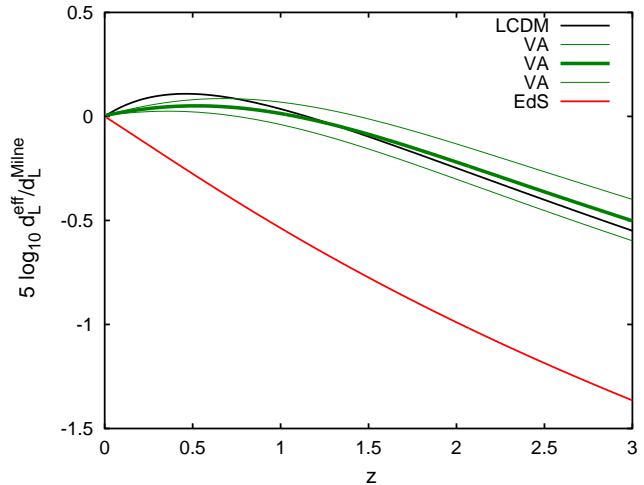


FIG. 5. (colour online) Distance moduli for the EdS (bottom curve) and Λ CDM (top curve for $z \lesssim 0.5$, black online) homogeneous models, and for the EdS virialization approximation (Sect. II; green online, thick curve for $H_{\text{pec}}^{\text{com}}(0) = 36$ km/s/Mpc, thin curves for $H_{\text{pec}}^{\text{com}}(0) = 33$ and 39 km/s/Mpc), all normalized to the Milne model ($\Omega_{m0} = 0 = \Omega_{\Lambda0}$).

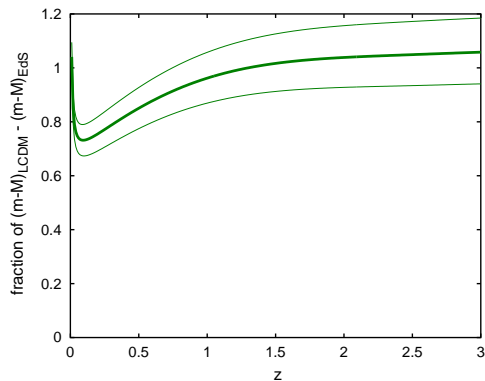


FIG. 6. Fraction of EdS-to- Λ CDM distance modulus f_{m-M} (42) provided by the virialization approximation.

element needed to match faint number counts is provided by this approximation.

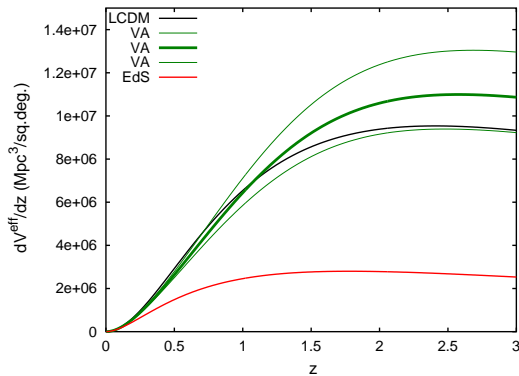


FIG. 7. (colour online) Differential volume element dV^{eff}/dz (41) for the EdS (bottom curve) and Λ CDM (black online) homogeneous models and for the EdS virialization approximation (thick and very thin curves for $H_{\text{pec}}^{\text{com}}(0) = 39, 36$, and 33 km/s/Mpc, from top to bottom, respectively, green online), in comoving $\text{Mpc}^3/\text{sq.deg}$.

IV. DISCUSSION

The dominance of negative curvature over positive curvature on large scales at recent epochs has already been postulated based on detailed kinematical and curvature backreaction estimates [23] and models [16, 25, 40, 50–55]. By definition, over- and under-densities of comoving perturbations in an FLRW background model average to zero. In general, this is also true on mass-preserving Lagrangian domains \mathcal{D} in the nonlinear regime. The restmass conservation law assures compensation to hold throughout the evolution of structure. However, the intrinsic curvature does not obey a conservation law: only a dynamical relation between the kinematical backreaction, curvature, and volume evolution is conserved [23], as is used in this paper through (3) with $\Omega_\Lambda = 0$; see the discussion in [52].

Virialized regions are, by definition, highly concentrated, occupying very little volume. Thus, while the average of the density deviations from the background tends to zero, the average peculiar curvature (average curvature with respect to the background FLRW model curvature) tends to a negative value when a high fraction of matter has virialized. The key formula in [23] is (104), with a general discussion in Section 5 of strategies for calculating a more detailed approximation than the one presented here.

At small enough scales, the backreaction model based on a volume average of the relativistic Zel’dovich approximation mentioned above, representing the effects of the statistical formation of structure in detail [24, 25], shows that positive curvature dominates in collapsing regions. It is speculated that, on these smaller scales, positive curvature plays the role that is usually attributed to “dark matter”, i.e. that a substantial portion of dark matter might also be an artefact of using a Newtonian approxi-

mation to structure formation. Although the estimates in this paper deal with void scales and larger, detailed relativistic calculations would have to take this into account. We do not attempt to model this here, since we consider our results to be an initial quantitative estimate of an important physical effect, suggesting that it is worthwhile to go beyond the model presented here.

For over a decade, radially inhomogeneous models, both Stephani [56] and LTB [57, 58] models, have been proposed as dark-energy-free, relativistic fits to the type Ia supernovae luminosity-distance-redshift relation, and have become best known as “void models” [59, 60] on a scale of up to ~ 2.5 Gpc (e.g., [61]), although “hump models” have also been inferred from the data [29, 30]. There has been much debate over whether or not the fits should be excluded on either observational grounds or as being in conflict with the Cosmological Principle. (See, e.g., [62].)

The virialization approximation (which is neither a Stephani nor an LTB model) suggests another interpretation that may resolve some issues in these debates. It is true that in a comoving, constant time slice at the present epoch t_0 , a reasonable projection of our past light cone observations forward to t_0 is hard to reconcile—at least for large-scale homogeneous models—with our location near the centre of a void as large as a gigaparsec. However, cosmological observations are not made on the t_0 time slice. *On the past light cone*, the virialization epoch approximately corresponds to an observer-centred “void” of a gigaparsec or so in size, where “void” here means, e.g., the spherical region around the observer extending over the redshift range where $f_{\text{vir}}(z) \gtrsim 0.1$. The “void” that is relevant for an effective metric is that defined by the volume-averaged density parameter on our past light cone, and this “void” is mirrored by virialization. We are located at a highly privileged, highly non-random, centralized position on the past light cone: at the apex of the cone, which is the epoch of highest virialization. Thinking spatially at constant t , locating the observer at the centre of a (non-averaged) void is a hypothesis, while on the past light cone, our privileged position is a geometrical fact.

With hindsight, the *numerical* results of LTB void models by, e.g., [63] and the LTB void model $H_0(r)$ estimates of [64], for a radial coordinate r at constant cosmological time, roughly correspond to the results found here, but with fundamental differences in their derivation and interpretation. Here, we start with a large-scale homogeneous (EdS) model and use standard N -body simulations to quantify an approximate, effective metric at low redshifts, providing a general-relativistic correction to the FLRW metric. Our resulting “void” is a past-light-cone, virialization-epoch, volume-averaged pseudo-void only. In the LTB models, H_0 and Ω_{m0} vary with the radial coordinate r at a constant cosmological time t , at which there is a true void rather than a virialization-epoch “void”. However, the LTB model parameters are motivated by and interpreted in relation to

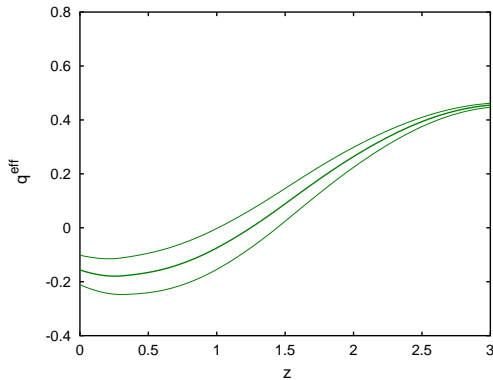


FIG. 8. Effective deceleration parameter q^{eff} (43) for the EdS virialization approximation presented in this paper.

observations—on the past light cone. Thus, it is unsurprising that the numerical results are roughly similar to ours.

A more closely related inhomogeneous, dark-energy-free relativistic model is the timescape model (formerly known as the “fractal bubble” model) [65–67]. At late epochs, this is a negatively-curved, void-dominated, multi-scale, scalar averaging model that focuses particularly on time calibration. The model compares well to the Λ CDM model in fitting supernovae type Ia data [68] and has been used to interpret bulk velocity flows on scales up to $65 h^{-1}$ Mpc from the Local Group [69].

Is the scale factor accelerating according to the virialization approximation? The study of LTB models shows that for inhomogeneous universe models in general, at least two different definitions of the deceleration parameter can be usefully made, and luminosity-distance-redshift observations do not imply model-free estimates of either of these [70]. Here, using the path of a radial photon in (38), $d\chi^{\text{eff}}/da$ from (39), and appropriately converting between space and time units, an effective deceleration parameter,

$$q^{\text{eff}}(z) := -\frac{\ddot{a}a}{\dot{a}^2}, \quad (43)$$

can be defined. Figure 8 shows that for this definition, moderate acceleration occurs for $z \lesssim 1.5$.

Given that only two observational values are used in the above approximation, i.e. one that is commonly derived from observations, $H^{\text{eff}}(0)$ (28), and one that we derive here from observations, $H_{\text{pec}}^{\text{com}}(0)$ (37), it would be to see if the approximation agreed with other further observational constraints beyond $\Omega_{\text{m}}^{\text{eff}}(0) = 0.26 \pm 0.05$ and the $d_L^{\text{eff}}(z)$ relation. One important constraint is the age of the Universe at the (approximately comoving) observer’s spacetime location. Using the EdS age at $z = 10$, the virialization approximation gives the present-day age of the Universe $t_0 = 12.2_{-0.4}^{+0.6}$ Gyr. This is a little low, but consistent with $t_0 = 13_{-2}^{+4}$ Gyr from the stellar population dating of moderate redshift elliptical galaxies over

$0.3 < z < 0.9$ [71], or $t_0 \gtrsim 12.8 \pm 1$ Gyr from globular cluster ages calibrated using Hipparcos parallaxes [72].

V. CONCLUSION

The approximation presented above assumes “old physics” (general relativity), not “new physics”. It is a rough approximation of old physics, general relativity, applied to the old observations of a high virialization fraction (galaxies, clusters of galaxies) at recent epochs and at a small distance scale in the past light cone. Numerical values of $f_{\text{vir}}(z)$ are estimated from a standard EdS N -body simulation [18, 19]. Only two observational values are assumed: the zero-redshift Hubble parameter (28) and the zero-redshift peculiar expansion rate across non-virialized regions, $H_{\text{pec}}^{\text{com}}(0)$ (37). The inferred effective low redshift matter density parameter is realistic, $\Omega_{\text{m}}^{\text{eff}} = 0.26 \pm 0.05$, and the virialization-corrected EdS distance modulus is close to the Λ CDM distance modulus (Figs 5, 6).

Of course, virialized objects cannot be completely ignored, the virialization fraction is derived from an N -body simulations with a fixed (zero) curvature EdS model, and different choices of parameters in the N -body analysis (group finder algorithm, group finder minimum number of particles, definition of the void size) and the N -body simulation itself (calculation algorithm, volume of the simulation, particle mass resolution) would be likely to modify the above calculations. Our proposed interpolation (29) and normalization (37) of $H_{\text{pec}}^{\text{com}}(z)$ could also be improved in many ways. It is, however, unlikely that these refinements would substantially reduce the amplitude of the corrections estimated here, since the observational evidence in favor of a high virialization fraction at the present epoch $z \ll 1$ and the observational and theoretical evidence for $H(z) + H_{\text{pec}}^{\text{com}}(z) a^{-1}$ (24) to roughly follow the values shown in Fig. 3 is strong. A more detailed approximation than that presented here might show that a hyperbolic or spherical, zero-dark-energy background FLRW metric, corrected for virialization, would better match the full range of observational constraints. It may also be important to consider inhomogeneous light-path effects on standard candles, such as type Ia supernovae, as a bias when assuming the FLRW models as a family of background models [73–75]. High redshift observations should be modeled and interpreted in a way that avoids dependence on the low redshift metric. Low-redshift peculiar-velocity observations (e.g. [76]) would be useful if designed to optimally estimate $H_{\text{pec}}^{\text{com}}(0)$.

Pending more accurate, relativistic calculations, it would seem prudent to consider “dark energy” as an artefact of virialization-induced negative spatial curvature and void-dominated expansion rates, both of these being physical properties that are neglected in the standard cosmological framework.

ACKNOWLEDGMENTS

Thank you to Martin Kerscher, Tomasz Kazimierczak Alexander Wiegand, Bruce A. Peterson, and Bartosz Lew for useful comments. Some of this work was carried out within the framework of the European Associated Laboratory “Astrophysics Poland-France”. BFR thanks the Centre de Recherche Astrophysique de Lyon for a warm welcome and scientifically productive hospitality. A part of this work was conducted within the “Lyon Institute of Origins” under grant ANR-10-LABX-66. Some of JJO’s contributions to this work were supported by the Polish Ministry of Science and Higher Education under “Mobilność Plus II edycja”. A

part of this project has made use of Program Obliczeń Wielkich Wyzwań nauki i techniki (POWIEW) computational resources (grant 87) at the Poznań Supercomputing and Networking Center (PCSS). The N -body simulations analyzed in this paper were carried out by the Virgo Supercomputing Consortium using computers based at the Computing Centre of the Max-Planck Society in Garching and at the Edinburgh Parallel Computing Centre[77]. Use was made of the GNU OCTAVE command-line, high-level numerical computation software (<http://www.gnu.org/software/octave>), and the Centre de Données astronomiques de Strasbourg (<http://cdsads.u-strasbg.fr>).

-
- [1] M. Fukugita, K. Yamashita, F. Takahara, and Y. Yoshii, *ApJL* **361**, L1 (Sep. 1990)
- [2] Y. Yoshii and B. A. Peterson, *Astrophys. J.* **444**, 15 (May 1995)
- [3] M. Chiba and Y. Yoshii, *Astrophys. J.* **489**, 485 (Nov. 1997)
- [4] B. Fort, Y. Mellier, and M. Dantel-Fort, *A&A* **321**, 353 (May 1997)
- [5] S. Perlmutter, G. Aldering, G. Goldhaber, et al., *Astrophys. J.* **517**, 565 (Jun. 1999), arXiv:astro-ph/9812133
- [6] B. P. Schmidt, N. B. Suntzeff, M. M. Phillips, et al., *Astrophys. J.* **507**, 46 (Nov. 1998), arXiv:astro-ph/9805200
- [7] D. N. Spergel, L. Verde, H. V. Peiris, et al., *ApJS* **148**, 175 (Sep. 2003), astro-ph/0302209
- [8] Planck Collaboration, P. A. R. Ade, N. Aghanim, C. Armitage-Caplan, M. Arnaud, M. Ashdown, F. Atrio-Barandela, J. Aumont, C. Baccigalupi, A. J. Banday, and et al., ArXiv e-prints(Mar. 2013), arXiv:1303.5076
- [9] W. de Sitter, *MNRAS* **78**, 3 (Nov. 1917)
- [10] A. Friedmann, *Mir kak prostranstvo i vremya (The Universe as Space and Time)* (Petrograd: Academia, 1923)
- [11] A. Friedmann, *Zeitschr. für Phys.* **21**, 326 (1924)
- [12] G. Lemaître, *Annales de la Société Scientifique de Bruxelles* **47**, 49 (1927)
- [13] H. P. Robertson, *Astrophys. J.* **82**, 284 (Nov. 1935)
- [14] T. Buchert, *General Relativity and Gravitation* **40**, 467 (Feb. 2008), arXiv:0707.2153
- [15] E. W. Kolb, V. Marra, and S. Matarrese, *General Relativity and Gravitation* **42**, 1399 (Jun. 2010), arXiv:0901.4566
- [16] J. Larena, J.-M. Alimi, T. Buchert, M. Kunz, and P.-S. Corasaniti, *Phys. Rev. D* **79**, 083011 (Apr. 2009), arXiv:0808.1161
- [17] T. Buchert, G. F. R. Ellis, and H. van Elst, *General Relativity and Gravitation* **41**, 2017 (Sep. 2009), arXiv:0906.0134
- [18] A. Jenkins, C. S. Frenk, F. R. Pearce, P. A. Thomas, J. M. Colberg, S. D. M. White, H. M. P. Couchman, J. A. Peacock, G. Efstathiou, and A. H. Nelson, *Astrophys. J.* **499**, 20 (May 1998), arXiv:astro-ph/9709010
- [19] P. A. Thomas, J. M. Colberg, H. M. P. Couchman, et al., *MNRAS* **296**, 1061 (Jun. 1998)
- [20] J. P. Ostriker and P. J. Steinhardt, ArXiv Astrophysics e-prints(May 1995), arXiv:astro-ph/9505066
- [21] C. Lacey and S. Cole, *MNRAS* **262**, 627 (Jun. 1993)
- [22] T. Buchert, M. Kerscher, and C. Sicka, *Phys. Rev. D* **62**, 043525 (Aug. 2000), arXiv:astro-ph/9912347
- [23] T. Buchert and M. Carfora, *Classical and Quantum Gravity* **25**, 195001 (Oct. 2008), arXiv:0803.1401
- [24] T. Buchert and M. Ostermann, *Phys. Rev. D* **86**, 023520 (Jul. 2012), arXiv:1203.6263
- [25] T. Buchert, C. Nayet, and A. Wiegand, *Phys. Rev. D*, in press (Mar. 2013), arXiv:1303.6193
- [26] G. Lemaître, *Annales de la Société Scientifique de Bruxelles* **53**, 51 (1933)
- [27] R. C. Tolman, *Proceedings of the National Academy of Science* **20**, 169 (Mar. 1934)
- [28] H. Bondi, *MNRAS* **107**, 410 (1947)
- [29] M. Célérier, K. Bolejko, and A. Krasiński, *A&A* **518**, A21 (Jul. 2010), arXiv:0906.0905
- [30] E. W. Kolb and C. R. Lamb, ArXiv e-prints(Nov. 2009), arXiv:0911.3852
- [31] <http://arXiv.org/abs/1303.4444>
- [32] B. F. Roukema, P. J. Quinn, and B. A. Peterson, in *Observational Cosmology: an International Symposium, Milano, Italy, 21–25 September 1992*, Astronomical Society of the Pacific Conference Series, Vol. 51, edited by G. L. Chincarini, A. Iovino, T. Maccacaro, & D. Maccagni (1993) p. 298
- [33] B. F. Roukema, B. A. Peterson, P. J. Quinn, and B. Rocca-Volmerange, *MNRAS* **292**, 835 (Dec. 1997), arXiv:astro-ph/9707294
- [34] C. Lacey and S. Cole, in *Observational Cosmology: an International Symposium, Milano, Italy, 21–25 September 1992*, Astronomical Society of the Pacific Conference Series, Vol. 51, edited by G. L. Chincarini, A. Iovino, T. Maccacaro, and D. Maccagni (1993) p. 192
- [35] B. F. Roukema, S. Ninin, J. Devriendt, F. R. Bouchet, B. Guiderdoni, and G. A. Mamon, *A&A* **373**, 494 (Jul. 2001), arXiv:astro-ph/0105152
- [36] <http://www-hpcc.astro.washington.edu/tools/fof.html>
- [37] J. Tinker, A. V. Kravtsov, A. Klypin, K. Abazajian, M. Warren, G. Yepes, S. Gottlöber, and D. E. Holz, *Astrophys. J.* **688**, 709 (Dec. 2008), arXiv:0803.2706
- [38] M. White, *A&A* **367**, 27 (Feb. 2001),

- arXiv:astro-ph/0011495
- [39] M. White, *ApJSupp* **143**, 241 (Dec. 2002), arXiv:astro-ph/0207185
- [40] A. Wiegand and T. Buchert, *Phys. Rev. D* **82**, 023523 (Jul. 2010), arXiv:1002.3912
- [41] P. J. E. Peebles, *Large-Scale Structure of the Universe* (Princeton University Press, —c1980, 1980)
- [42] A. G. Riess, L. Macri, S. Casertano, H. Lampeitl, H. C. Ferguson, A. V. Filippenko, S. W. Jha, W. Li, R. Chornock, and J. M. Silverman, *Astrophys. J.* **730**, 119 (Apr. 2011), arXiv:1103.2976
- [43] W. L. Freedman, B. F. Madore, V. Scowcroft, C. Burns, A. Monson, S. E. Persson, M. Seibert, and J. Rigby, *Astrophys. J.* **758**, 24 (Oct. 2012), arXiv:1208.3281
- [44] M. Plionis and S. Basilakos, *MNRAS* **330**, 399 (Feb. 2002), arXiv:astro-ph/0106491
- [45] C. Foster and L. A. Nelson, *Astrophys. J.* **699**, 1252 (Jul. 2009), arXiv:0904.4721
- [46] K. Rines, M. J. Geller, M. J. Kurtz, and A. Diaferio, *AJ* **126**, 2152 (Nov. 2003), arXiv:astro-ph/0306538
- [47] N. Kaiser, *MNRAS* **227**, 1 (Jul. 1987)
- [48] A. Mazure, P. Katgert, R. den Hartog, et al., *A&A* **310**, 31 (Jun. 1996), arXiv:astro-ph/9511052
- [49] J. A. L. Aguierri, R. Sánchez-Janssen, and C. Muñoz-Tuñón, *A&A* **471**, 17 (Aug. 2007), arXiv:0704.1579
- [50] S. Räsänen, *Classical and Quantum Gravity* **28**, 164008 (Aug. 2011), arXiv:1102.0408
- [51] T. Buchert, *Classical and Quantum Gravity* **28**, 164007 (Aug. 2011), arXiv:1103.2016
- [52] T. Buchert and S. Räsänen, *Annual Review of Nuclear and Particle Science* **62**, 57 (Nov. 2012), arXiv:1112.5335
- [53] D. L. Wiltshire, *Classical and Quantum Gravity* **28**, 164006 (Aug. 2011), arXiv:1106.1693
- [54] X. Roy and T. Buchert, *Classical and Quantum Gravity* **27**, 175013 (Sep. 2010), arXiv:0909.4155
- [55] C. Clarkson, G. Ellis, J. Larena, and O. Umeh, *ArXiv e-prints*(Sep. 2011), arXiv:1109.2314
- [56] M. P. Dabrowski and M. A. Hendry, *Astrophys. J.* **498**, 67 (May 1998), arXiv:astro-ph/9704123
- [57] N. Mustapha, C. Hellaby, and G. F. R. Ellis, *MNRAS* **292**, 817 (Dec. 1997), arXiv:gr-qc/9808079
- [58] M.-N. Célérier, *ArXiv Astrophysics e-prints*(Jul. 1999), arXiv:astro-ph/9907206
- [59] K. Tomita, *MNRAS* **326**, 287 (Sep. 2001), arXiv:astro-ph/0011484
- [60] K. Bolejko, M.-N. Célérier, and A. Krasinski, *Classical and Quantum Gravity* **28**, 164002 (Aug. 2011), arXiv:1102.1449
- [61] J. Garcia-Bellido and T. Haugbølle, *JCAP* **4**, 003 (Apr. 2008), arXiv:0802.1523
- [62] A. Krasinski and K. Bolejko, *ArXiv e-prints*(Dec. 2012), arXiv:1212.4697
- [63] H. Alnes, M. Amarzguioui, and Ø. Grøn, *Phys. Rev. D* **73**, 083519 (Apr. 2006), arXiv:astro-ph/0512006
- [64] K. Enqvist, *General Relativity and Gravitation* **40**, 451 (Feb. 2008), arXiv:0709.2044
- [65] D. L. Wiltshire, *New Journal of Physics* **9**, 377 (Oct. 2007), arXiv:gr-qc/0702082
- [66] D. L. Wiltshire, *Physical Review Letters* **99**, 251101 (Dec. 2007), arXiv:0709.0732
- [67] D. L. Wiltshire, *Phys. Rev. D* **80**, 123512 (Dec. 2009), arXiv:0909.0749
- [68] P. R. Smale and D. L. Wiltshire, *MNRAS* **413**, 367 (May 2011), arXiv:1009.5855
- [69] D. L. Wiltshire, P. R. Smale, T. Mattsson, and R. Watkins, *ArXiv e-prints*(Jan. 2012), arXiv:1201.5371
- [70] K. Bolejko and L. Andersson, *JCAP* **10**, 003 (Oct. 2008), arXiv:0807.3577
- [71] I. Ferreras, A. Melchiorri, and J. Silk, *MNRAS* **327**, L47 (Nov. 2001), arXiv:astro-ph/0105384
- [72] L. M. Krauss, *Phys. Rep.* **333**, 33 (Aug. 2000), arXiv:astro-ph/9907308
- [73] K. Kainulainen and V. Marra, in *American Institute of Physics Conference Series*, American Institute of Physics Conference Series, Vol. 1241, edited by J.-M. Alimi and A. Fuözfa (2010) pp. 1043–1050, arXiv:0911.5584
- [74] C. Clarkson, G. F. R. Ellis, A. Faltenbacher, R. Maartens, O. Umeh, and J.-P. Uzan, *MNRAS* **426**, 1121 (Oct. 2012), arXiv:1109.2484
- [75] P. Fleury, H. Dupuy, and J.-P. Uzan, *ArXiv e-prints*(Feb. 2013), arXiv:1302.5308
- [76] R. B. Tully, E. J. Shaya, I. D. Karachentsev, H. M. Courtois, D. D. Kocevski, L. Rizzi, and A. Peel, *Astrophys. J.* **676**, 184 (Mar. 2008), arXiv:0705.4139
- [77] <http://www.mpa-garching.mpg.de/NumCos>